Cyber-Physical System for Gait Analysis and Fall Risk Evaluation by Embedded Cortico-muscular Coupling Computing

V. F. Annese, G. Mezzina, D. De Venuto,
Politecnico di Bari, Dept. of Electrical and Information Engineering (DEI)
Via Orabona 4, 70125 Bari – Italy
{valeriofrancesco.annese, daniela.devenuto}@poliba.it; g.mezzina23@gmail.com

***Abstract*— The paper describes the architecture of a non-invasive, wireless embedded system for gait analysis and preventing involuntary movements including falls. The system operates with synchronized and digitized data samples from 8 EMG (limbs) and 8 EEG (motor-cortex) channels. An embedded Altera Cyclone V FPGA operates the real-time signal pre-processing and the computation (resource utilization: 85.95% ALMs, 43283 ALUTs, 73.0% registers, 9.9% block memory; processing latency < 1ms). The system has been tested on patients affected by Parkinson disease (PD) under physician guide and compared with healthy subjects' results. Both PD and healthy subjects have been involved in the standard diagnostic protocol (normal gait and pull test). The developed cyber-physical system detects differences between the PD and the healthy subjects in terms of walking pattern, i.e., agonist-antagonist co-contractions (Typ time: PD's 148ms vs Healthy 88ms; Max: PD's 388ms vs Healthy 314ms). The PD's cerebral Movement Related Potentials (i.e., Bereitschaft) analysis during the pull-test showed an increasing from 59dBμ to 66dBμ after 3 settling steps while measurements on healthy subject return, respectively, 57dBμ, 62dBμ in 1 settling step. The system is able to prevent fall enabling the actuator in 168ms, i.e., better than the normal human time reaction (300ms).**

Keywords-Fall prevention; EEG; EMG; MRPs; FPGA.

I. INTRODUCTION

Due to neurological diseases, muscular deformities, ageing and further numerous factors, the normal gait frequently tends to degenerate into gait disorders. They constitute a contributive intrinsic falling cause, heavily increasing the risk of falling. Nowadays, 28–35% of people aged 65 years and above fall and, as consequence, each year more than 424000 fall events are fatal [1][2]. The economic impact of this phenomenon is impressive: 43.8 billion dollars are estimated to be used in fall-related medical care expenditures by 2020 [3]. Despite the extensive research in this field, developed tools for fall risk have not been successful in predicting and preventing falls [3]. Indeed, although fall detection technology is now mature (detectors for domestic use can be implemented using artificial vision techniques, tri-axial gyroscopes and accelerometers, Microsoft Kinect's infrared sensors, floor vibrations and sounds and numerous others) [4], fall prevention solutions are still far to be implemented. Fall prevention systems can be mainly divided into four categories: static fall-risk assessment, pre-fall intervention, fall-injury prevention and fall prevention [5][6]. The static fall-risk assessment category includes all the protocolled clinical tools which aim to identify people with high fall-risk due to neuro-muscular diseases (i.e., Barthel Index [7], the TGBA index [8], STRATIFY [9], TUG [10]). The static fall-risk assessment tools are indispensable for the beginning of a drug/rehabilitation plan but do not perform any intervention for preventing falls. The pre-fall intervention category includes all the methods oriented to the improvement of balance, stability and muscular strength of the subject. In recent years, in order to create more appealing exercises, assistive technology has been successfully implemented to drive the patients into a kind of game-exercise (i.e., Microsoft Kinect, Nintendo Wii, VR tools [11][12]). They can be part of a wider preventive plan but they cannot constitute a standalone solution since they do not limit the consequent damage of a fall. The fall-injury prevention category groups all the technologies implementing a shock absorber when a fall event is detected. Those systems are made up by the fall detection system and by the actuator, which timely manage the shock absorber. The shock absorption is conducted by an airbag that is promptly inflated. Toshiyo et al. [13] present a system protection against impact with the ground using accelerometers and gyroscopes for the fall detection and a jacket-worn airbag to be timely inflated before the impact. These systems, although reduce effectively the damage due to the fall, fail to cover all the scenarios and do not limit the brain damage associated with it (i.e., fair of falling). The fall prevention category aims to definitively avoid the fall event [14-17]. In [14], Zeilig et al., describe a fall prevention system named "ReWalk" consisting of a multi-sensing platform (blood pressure, ECG, etc.) for fall detection combined to an exoskeleton to assist the movement of the subject. Vuillerme et al. [15] propose to use a combination of pressure sensors and electro-tactile biofeedback to prevent the fall. Additionally, Munro et al. [16] describe a fall prevention tool based on an intelligent wearable knee flexion controller. These systems are the most suitable for fall prevention since if a fall event is detected, a feedback aiming to correct the movement is delivered to the subject and the fall is avoided. In this frame, we propose a novel digital back-end architecture for fall prediction in the everyday life. The architecture, implemented on a field programmable gate array (FPGA), combines both electroencephalography (EEG) and electromyography to take decision for processing and eventual corrective actions on the muscles. To the best of our knowledge, our architecture is the first fully implemented cyber-physical system, which allows fall prevention by real-time processing of coupled EMG and EEG.

 ISBN: 978-1-61208-507-4

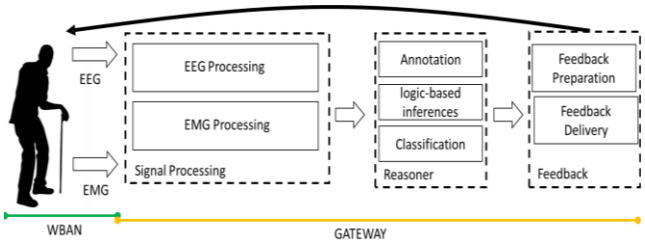

Figure 1. Architecture of the proposed system.

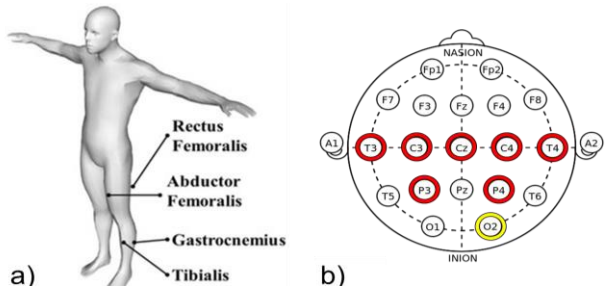

Figure 2. EMG (a) and EEG (b) electrodes setting

The paper is structured as follows. Section II introduces basic medical knowledge for the fall prediction. Section III discusses the cyber-physical system architecture. Section IV presents experimental data from a Parkinson's diseased (PD) patient and a healthy subject.

II. MEDICAL BACKGROUND

Literature studies demonstrate the possibility to predict a fall by a combined analysis of muscular movement (EMG) and its brain pre-processing (EEG) by monitoring EEG Movement Related Potentials (MRP) anticipating muscle activations [1-4, 17-18]. Currently none of the above remarked solutions enables such analysis: indeed only partial solutions have been proposed in literature. In fact, some systems measure individually EEG or EMG; others measure both of them, but only on a few EEG/EMG electrodes without relative synchronization, using an external clock and delivering filtered data to be post-processed and not handled in real time [19]. We mainly focus on Bereitschaftspotential (BP), μ and β rhythms that can be detected in the motor-cortex area even one second before the muscle activation in the band of 2–5Hz, 7–12Hz, and 13–30Hz respectively. In movement disorders, mobility impairment is indicated by an altered modulation of the MRPs as well as a mismatch between the MRPs and the movement. EMG data are processed in parallel, aiming to evaluate the co-contraction time among agonist-antagonist muscles. The co-contraction time is the period during which an agonist and antagonist muscles (i.e., Gastrocnemius and Tibialis) are contracted at the same time. During normal gait where agonist and antagonist muscles are alternately activated, the co-contraction time is low (< 300ms) and depends on the particular subject. High EMG co-contraction time during gait (larger than 500/600ms depending on the subject) is a significant index of unbalance and instability. According to [20], a reaction time of 300ms or lower returns a probability $p < 0.01$ of falling. Therefore, if the system reacts within this time limit and delivers a corrective action, the fall can be avoided.

III. THE CYBER-PHYSICAL SYSTEM

The high-level architecture of the cyber-physical system is outlined in Fig. 1. The wireless body area network (WBAN) allows synchronized collection of EEG and EMG. Eight EEG (according to the international 10-20 system T3, T4, C3, C4, CZ, P3, P4, O2, – 500Hz and 24bit resolution) and as many EMG channels (Gastrocnemius, Tibialis, Rectus and Biceps Femoralis of both the legs – 500Hz sampling rate and 16bit resolution [21]) are collected by a wireless and wearable recording systems, and sent to a gateway as shown in Fig. 2. The signal processing is performed on an FPGA. Signal processing outcomes are subsequently passed to a reasoner, which detect critical situation by analyzing EEG, EMG, inertial sensor data, environment and clinical condition information. When a potential fall is detected, a feedback is generated and delivered to the subject. The global vision of the project includes the electrical stimulation of the antagonist limb muscles in order to favor the postural correction, drastically reducing the probability of fall. The electrostimulation sub-system is part of our future works.

A. High-Level Algorithm Description

EMG and EEG follow two different processing branches. A trigger signal is extracted from EMG raw data using a dynamic-threshold approach. The trigger signal is computed as follows. First, the EMG signal is rectified, squared and stored in an M samples shift-register (in our algorithm M = 512, that is 1s data). The mean value of all register samples (global average) is therefore directly the EMG power in the M samples window and it is used as threshold. A second mean value (local average) is computed on the last N samples (i.e., corresponding to just a part of the complete M samples shift register, being N<M, in our design N = 128) and compared with the threshold. As a new EMG sample arrives, both global and local average are refreshed, making the thresholding scheme dynamic. The EMG trigger rises and stays high only if the local power is larger than the dynamic global average threshold. This approach heavily compresses the EMG signals, providing and unambiguous muscle activation signal (only 1bit trigger signal per muscle). For the EEG part running in parallel with respect to the EMG one, the time-frequency analysis is run on seven motor-cortex channels only (T3, T4, C3, C4, CZ, P3, P4), while the occipital one (O2) is used for noise reduction. As soon as new EEG samples arrive, data are stored in a 256 samples register. When a coupled EMG rising edge is detected, a 256 points 24bit resolution Fast Fourier Transform (FFT) is computed on the previous 256 EEG samples stored into the register. The cortical involvement is opposite with respect to the movement performed: if a right limb movement is detected (right

 ISBN: 978-1-61208-507-4

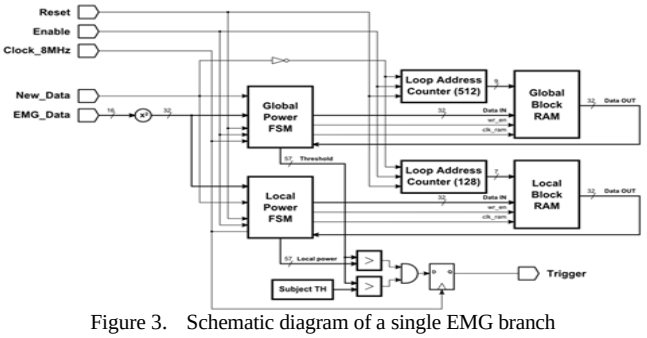

Figure 3. Schematic diagram of a single EMG branch

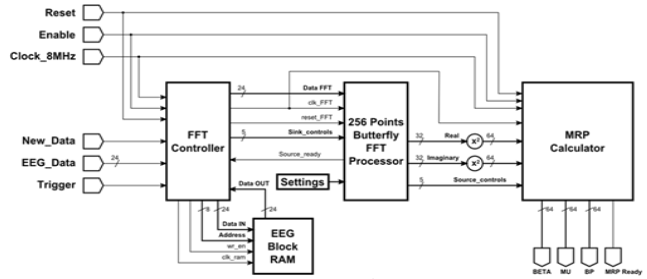

Figure 4. Schematic diagram of a single EEG branch

Gastrocnemius), the analysis is performed on left motor-cortex channels (Cz, C3, T3, P3) and vice versa (left Gastrocnemius triggers Cz, C4, T4, P4, note that since Cz is a central channel is triggered by both). The FFT output data are processed to compute the square magnitude and the appropriate frequency components summed in order to calculate the spectral powers in the MRPs bands. When the EMG trigger arrives, the EEG power levels in the MRPs band are referred to approximately 500ms before the movement occurs. The obtained power levels for each EEG channel are then compared to fixed thresholds (which need to be trimmed on the subject) in order to evaluate the voluntariness of the EMG contraction. Thresholds are customized on the individual after a period of learning (the subjects were asked to rest for 1 minute).

B. FPGA Architecture: Processor System-level Design

In the aim of a future ASIC implementation, the architecture has been validated on a FPGA (Altera Cyclone V). A more detailed description of the FPGA implementation has been presented in [21][22]. The input-output interface of our design is characterized by:16 bio-signals inputs (eight 16bit EMG and eight 24bit EEG); 25 outputs (BP, μ and β 1bit flags for the seven EEG motor-cortex channels and 4 co-contraction 1bit signals). The System clock is set to 8.19209MHz (signal `8 MHz CLK`), obtained with an on-chip Phase-Locked Loop (PLL, block named `PLL`) from the embedded 50MHz oscillator (`50 MHz CLK`). The global signals of the whole implementation are: `Reset`, an asynchronous reset (derived from the `Reset KEY` input) ; `Enable SW`, an enable signal which freezes the processing; `500Hz CLK`, an input data clock signal from the EMG and EEG channels (500Hz frequency); `8 MHz CLK`, a 8.19209MHz system clock obtained by the on-chip PLL. In the complete system, 8 EMG and 7 EEG processing branches are replicated in parallel on the FPGA. In the following sub-section, we summarize the processing data path for a generic combined [21][22].

EMG Processing Branch (see Fig. 3). Incoming squared EMG samples passed to two FSMs, Global Power FSM and Local Power FSM, to calculate in parallel, respectively, the dynamic threshold (global power) and the local power. Based on two block RAM (Global Threshold and Local Threshold Block RAM of M = 512 and N = 128, 32bit words), when a new EMG sample arrives (500Hz CLK = '1') the last inserted sample is pointed and "pop" (512th and 128th for, respectively, `Global Power` and `Local Power Block RAM`). Then, the read sample is subtracted and the new sample is added to refresh the overall power `Sum` within the window. An asynchronous 64bit comparator (>) compares the powers calculated in parallel by the two blocks (`THR` and `Local THR`). `Local THR` is also compared to a fixed threshold (evaluated on the subject resting) that prevents unpredictable behavior due to noise when the subject stops walking. The output of the comparator is the 1bit EMG trigger (signal Trigger), used both in the EEG computation to enable the time-frequency analysis and in the co-contraction calculation. The co-contraction signal is obtained by computing an AND logic operation on agonist-antagonist coupled muscles. The adopted approach allows the efficient calculation of the powers in the desired windows, without necessarily having to re-compute, at each 8MHz clock rising edge, the overall sum of the RAMs.

EEG Processing Branch (see Fig. 4). The EEG branch comprises a 256 points 24bit resolution FFT processor based on a butterfly structure [24, 25]. The 256 EEG samples to be transformed are dynamically stored in a 256 24bit words RAM(`EEG Block RAM`) addressed by a loop address counter in the `FFT Controller`. When EMG Trigger rises to '1', the 256 samples stored into the RAM are passed the FFT block by properly temporizing the Sink_controls signals through a series of dedicated states. After data is sent and validated (Source_controls), the FSM waits for another Trigger rising edge to repeat the sequencing. The FFT output data is interpreted by the MRP Calculator where they are squared and opportunely summed (both real and imaginary parts) using a 64bit adder in order to extract the BP, μ and β powers, in natural units (BP, MU, BETA signals). Finally, when MRP Ready is asserted, BP, μ and β are compared to fixed thresholds related to the subject, preloaded on the FPGA.

C. The Reasoner

The decision algorithm is based on the annotation of EMG/EEG wireless wearable electrodes signals and on the application of logic-based inferences in order to classify fall patterns and calculate a response for feedback delivery.

 ISBN: 978-1-61208-507-4

EMG co-contractions, EEG MRPs and data acquired from an inertial sensor are used to distinguish when a fall is starting and to trigger the further processing steps. The environmental conditions and the medical history of the patient are taken into account. The reasoner has been already developed in previous works: a more detailed description of the semantic matchmaking algorithm is reported in [19].

IV. RESULTS

Experimental results on healthy subjects have been already presented in [21-23, 25, 31-33]. In the present paper, we propose a dataset including EEG/EMG recordings of a subject affected by Parkinson disease (PD) and a healthy one, both performing natural gait (120s) and 'pull tests' [26]. Those tests are performed in a controlled environment (local hospital), under the supervision of specialized staff. The use of the proposed system in these analyses provides a systematic and objective quantification of diagnostic indexes. Overall, the worst case power consumption (when unrealistically all blocks are simultaneously operating) can be estimated as 150mW, which is a feasible upper bound for portable applications [21, 24, 28, 29]. The system is able to deliver the corrective action in 168ms well within the 300ms time limit (data collection: 14ms; data processing: 42ms; reasoning: 12ms; feedback: 100ms) [19].

A. Cyber-Physiscal System Performance

The FPGA system implementation with 16 bio-signals inputs and 25 outputs requires 81.7% ALMs (arithmetic logic module), 44808 ALUTs, 73.4% registers, 10.3% block memory of the available resources. FPGA results present a mean relative error of 0.01% if compared with Matlab outcomes on the same dataset. The most power hungry part of the system is the FFT. In a 180nm CMOS ASIC, a 16bit butterfly 256 points FFT at 4MHz would consume about 13mW during continuous operation including block RAM, which at 4MHz would consume approximately 1mW [27].

B. Experimental Results: Gait Analysis

For the gait analysis, the subjects are asked to perform a natural and fluid walk. The results are summarized in table I, which reports, from the top of the table, the failure rate of the EMG trigger generation, maximum, typical and number/second co-contractions, limb muscles activation/deactivation and their ratio (duty cycle) during a single step. Table I distinctly shows the parameters for PD and healthy subjects. The results quantify the differences between the PD and the healthy subjects in terms of walking patterns.

i. The EMG trigger failure rate to detect EMG contraction is only 0.07% (worst-case).

ii. The Haste rate (HR), defined as number of co-contractions (ccs) per second, is 1.17 ccs/s for the PD subject against 0.44 ccs/s for a healthy subject: co-contractions are more frequent in PD than the healthy.

iii. Typical co-contraction times show an increase of 58ms (average value on all the four muscles couples) between PD subject and healthy one with greater incidence on the right leg (Δt=+120ms on R.Gast-R. Tib and Δt=+90ms on R. Bic – R. Rect): the co-contraction times are, on average, higher in PD than the healthy during gait.

iv. The maximum co-contraction time for the PD subject is higher for all the muscles if compared with the healthy subject (e.g. PD Max= 756ms and Healthy Max=548ms on L. Rect-L. Bic). The maximum co-contraction time is higher in PD than the healthy during gait.

v. On single muscle, PD subject shows contraction times that cover, on average, the 48.56% of the step time length. The healthy subject returns a value of 33.62%. The PD outlines muscular hyperactivity during gait. During normal gait, no significant differences on MRPs were found.

Indeed, both subjects present a BP that ranges from 58-65 dBμ, μ-rhythm ranges from 51-55 dBμ and β-rhythm sweeps between 41-44 dBμ. However, considering the BP, evident differences have been highlighted in both subjects between the state of resting and the time slot preceding the step. Considering the healthy subject, in the resting state the BP mean value was 49±4.6 dBμ while before a step the BP mean value reached 60.8±6.4 dBμ (see Fig. 5). The difference of the walking patterns is also evident from the diagram presented in Fig. 6, on which is reported a BP vs. co-contraction times plot for PD (in blue) and healthy (in red) subjects is shown. For clarity, the shown co-contraction times are computed on the left gastrocnemius/tibialis pair while the shown BP are referred to the right-motor

TABLE I. GAIT ANALYSIS OF A PD AND A HEALTHY SUBJECT ACHIEVED BY THE PROPOSED CYBER-PHYSISCAL SYSTEM

Parkinson's Diseased subject								
	L REC	L BIC	R TIB	R GAS	L TIB	L GAS	R REC	R BIC
Detection fails (%)	0.03	0.07	0.07	0.02	0.06	0.01	0.02	0.07
Co- contractions								
Max (ms)	756		630		446		640	
Typ (ms)	265.3±120.4		260.4±136		127.5±94		336.0±84	
Haste rate (num/s)	1,53 (184/120)		1,1 (132/120)		1.07 (129/120)		0,99 (119/120)	
Contractions								
Active (ms)	381±138	434±197	553±259	381±86	285±151	462±80	352±141	426±77
Deactive (ms)	232±124	329±157	260±129	696±139	997±366	637±153	208±123	673±110
Duty cycle (%)	62.2	56.9	68.0	35.4	22.3	42.1	62.8	38,8

Healthy subject								
	L REC	L BIC	R TIB	R GAS	L TIB	L GAS	R REC	R BIC
Detection fails (%)	0.02	0.03	0.06	0.02	0.04	0.01	0.02	0.03
Co- contractions								
Max (ms)	548		364		270		542	
Typ (ms)	268±138		140±103		100±55		246±140	
Haste rate (Num/s)	0.68 (82/120)		0.25 (30/120)		0.25 (30/120)		0.59 (71/120)	
Contractions								
Active (ms)	353 ±129	509 ±197	575 ±208	383 ±170	566 ±255	445 ±110	330 ±142	497 ±182
Deactive (ms)	1179 ±650	788 ±361	633 ±282	868 ±392	949 ±266	1010 ±228	1127 ±470	814 ±369
Duty cycle (%)	23.0	39.2	47.6	30.6	37.4	30.6	22.7	37.9

 ISBN: 978-1-61208-507-4

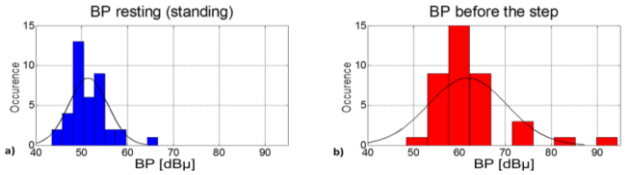

Figure 5. BP calculation in a resting state (a) and before the step (b).

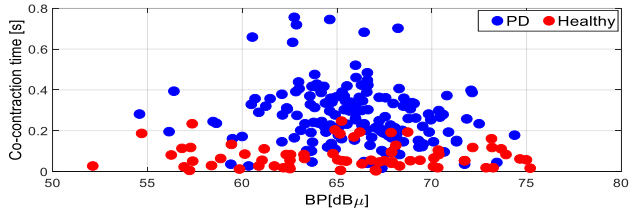

Figure 6. BP vs co-contraction time for both PD (blue) and healthy subjects (red).

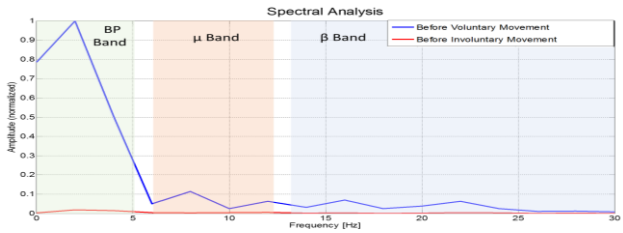

Figure 7. Normalized comparison between FFT computed on 500ms before a voluntary (blue) and involuntary (red) movement on Cz.

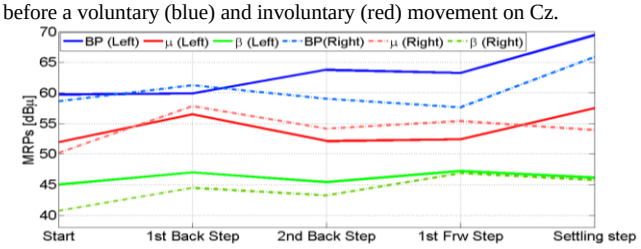

Figure 8. Demonstrative evidence of MRP power levels increment in the PD patient in order to recovery his stability.

TABLE II. MRPS AND CO-CONTRACTION VALUES DURING PULL TEST

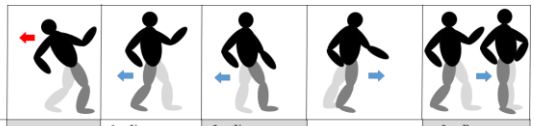

	START PULL TEST		1ST UNBALANCED STEP		2ND UNBALANCED STEP		1ST RECOVERY STEP		2ND RECOVERY STEP	
MRPS ON PARKINSON'S SUBJECT										
	R	L	R	L	R	L	R	L	R	L
BP(dBμ)	62.8	59.9	65	62.4	66	66.3	69.3	66	66	68.2
μ (dBμ)	49.6	54	54.5	54.7	55.4	55.7	55.8	57.9	57.6	59.5
β (dBμ)	46.06	45.6	46.33	44.26	48.16	43.7	44.58	47.9	46.27	47
MRPS ON HEALTHY SUBJECT										
	R	L	R	L	R	L	R	L	R	L
BP(dBμ)	58.40	56.40	-	-	-	-	69.20	64.20	-	-
μ (dBμ)	47.30	52.20	-	-	-	-	53.07	58.40	-	-
β (dBμ)	42.70	38.08	-	-	-	-	44.23	44.12	-	-

CO-CONTRACTIONS ON PARKINSON'S DISEASED SUBJECT DURING PULL TEST				
Max (ms)	L. RECT – L. BICEP	R. TIB – R. GAST	L. TIB – L. GAST	R. RECT – R. BICEP
	751	462	598.6	1060.6
CO-CONTRACTIONS ON HEALTHY SUBJECT DURING PULL TEST				
Max (ms)	L. RECT – L. BICEP	R. TIB – R. GAST	L. TIB – L. GAST	R. RECT – R. BICEP
	549	370	284	568

channels average. The analysis demonstrates that, while for the MRPs similar results are obtained for both subjects, the co-contractions for the PD subject are more frequent and reach values much higher in comparison with the healthy subject. In Fig. 7, a comparison between the EEG spectra computed before a voluntary movement (in blue) and before an involuntary movement (in red) are compared. The spectra are normalized. Considering the bands of interest (BP, μ and β), the power computed in the BP band during a voluntary movement is more than 100 times higher than the one calculated during an involuntary one. Similarly, the μ and β powers are about 10 times higher during a voluntary movement.

C. *Experimental Results: Pull Test*

The postural stability is tested in specialized centers by the "pull test" protocol [26]. During this test, the neurologist gives a moderately forceful backwards tug on the standing individual and observes how the person recovers his stability. The normal response is one or more quick backwards steps to prevent a fall. Usually during this test, the physician associates a numeric index basing on the subject response. Using the proposed cyber-physical system, we were able to quantify the instability of the subject and his intentionality in the stability recovery by MRPs. Pull test results for both PD and healthy subjects are summarized in Table II, which includes MRPs for both right (R) and left (L) EEG channels and the maximum co-contraction value reached. The EMG triggers analysis highlights that, when the sudden unbalancing is externally induced from the operator, PD subject reacted with four step. Two of these are backward, while two forward, until complete settling. The healthy subject reacted to the unbalancing with a single settling step. PD subject co-contractions in pull test increase, on average, of 98.75ms in comparison with gait's values. The healthy subject co-contraction values show no relevant change with an increase of 11.75ms. The PD subject co-contraction maximum value was 1.06s and was recorded on right biceps-rectus Femoralis. The MRPs have an interesting behavior when the sudden unbalancing happens. For the PD subject, MRPs increase their initial value (that sweep between 59.9-62.8dBμ) of 6.5dBμ on right EEG channels and 6dBμ on left ones. The increase is distributed over the steps showing the recovery of voluntariness during the movements. The healthy subject showed an initial range of 56.4-58.4dBμ and reached 64.2 dBμ (increase of 7.8 dBμ) and 69.2dBμ (increase of 7.8 dBμ) on left and right EEG channels respectively. The MRPs evolution during a single entire pull test for the PD subject is presented in Fig. 8. When the unbalance is externally induced, the recorded MRPs values are comparable to the resting values. However, in the subsequent recovery steps the MRPs increase both on right ($\Delta BP = +11.9\%$; $\Delta\mu = 5.5\%$; $\Delta\beta = +11.1\%$) and left ($\Delta BP = +14.3\%$; $\Delta\mu = +8.8\%$; $\Delta\beta = +2.2\%$) EEG channels.

V. CONCLUSION

In this work, a cyber-physical system for gait analysis and fall risk evaluation has been presented. EEG/EMG wireless nodes for real-time synchronous data collection make up the system. The system is able to evaluate different indexes, in order to establish the coupling between brain activity and movement, leading to the assessment of the intentionality level of a muscle contraction. An FPGA

(Altera Cyclone V) implementation, including test and validation of the system has been presented. The FPGA results show low residual numerical error (0.012%) if compared to Matlab ones and the maximum power consumption is of about 150mW. A further stage of semantic matchmaking collects, interprets and contextualizes the processed data. In this article, the system has been tested on a subject affected by the Parkinson's syndrome and on a healthy subject performing a natural gait and pull tests [28]. The system is able to detect critical conditions in 168ms (data collection: 14ms; data processing: 42ms; reasoning: 12ms; feedback: 100ms), within the 300ms, i.e., the standard time limit to avoid the fall [23].

REFERENCES

[1] World Health Organization. "Neurological Disorders. Public health challenges", Report., 2006

[2] M.E. Tinetti "Preventing falls in elderly persons", New England journal of medicine", 348.1:42–49, 2003.

[3] D. Oliver. "Falls risk-prediction tools for hospital inpatients. Time to put them to bed", Age Ageing, 37:248–50, 2008.

[4] Y. S. Delahoz et al. "Survey on fall detection and fall prevention using wearable and external sensors", Sensors: 19806–19842, 2014.

[5] M. De Tommaso, E. Vecchio, K. Ricci, A. Montemurno, D. De Venuto, V. F. Annese. "Combined EEG/EMG evaluation during a novel dual task paradigm for gait analysis." Proceedings - 2015 6th IEEE International Workshop on Advances in Sensors and Interfaces, IWASI 2015, art. no. 7184949, pp. 181-186. DOI: 10.1109/IWASI.2015.7184949. 2015.

[6] D. De Venuto and A.S. Vincentelli. "Dr. Frankenstein's dream made possible: Implanted electronic devices" Proceedings -Design, Automation and Test in Europe, DATE, art. no. 6513757, pp. 1531-1536. 2013.

[7] C. Collin et al. "The Barthel ADL Index: a reliability study." International disability studies. 2009.

[8] S. L. Vaught "Gait, balance, and fall prevention." The Ochsner Journal 3.2: 94-97. 2011.

[9] D. Oliver et al. "A systematic review and meta-analysis of studies using the STRATIFY tool for prediction of falls in hospital patients: how well does it work?." Age and ageing 37.6: 621-627. 2008.

[10] E. Nordin et al. "Prognostic validity of the Timed Up-and-Go test, a modified Get-Up-and-Go test, staff's global judgement and fall history in evaluating fall risk in residential care facilities." Age and ageing 37.4: 442-448. 2008.

[11] J. Hamm et al.. "Fall prevention intervention technologies: A conceptual framework and survey of the state of the art". Journal of Biomedical Informatics. 2016.

[12] M. Tinetti et al. "Fall risk index for elderly patients based on number of chronic disabilities." The American jour. of medicine 80.3,1986, 429-434.

[13] T. Toshiyo et al. "A wearable airbag to prevent fall injuries." Information Technology in Biomedicine, IEEE Transactions on 13.6: 910-914. 2009.

[14] Z. Gabi et al. "Safety and tolerance of the ReWalk™ exoskeleton suit for ambulation by people with complete spinal cord injury: A pilot study." The journal of spinal cord medicine 35.2: 96-101. 2012

[15] N. Vuillerme et al. "Pressure sensor-based tongue-placed electrotactile biofeedback for balance improvement-Biomedical application to prevent pressure sores formation and falls." Engineering in Medicine and Biology Society, 2007. EMBS 2007. 29th Annual International Conference of the IEEE. IEEE, 2007.

[16] B. J. Munro et al. "The intelligent knee sleeve: A wearable biofeedback device." Sens. Actuators B: Chemical 131:541. 2008.

[17] D. De Venuto, D. T. Castro, Y. Ponomarev, E. Stikvoort. "Low power 12-bit sar adc for autonomous wireless sensors network interface". 3rd International Workshop on Advances in Sensors and Interfaces, IWASI 2009, art. no. 5184780, pp. 115-120.DOI: 10.1109/IWASI.2009.5184780. 2009.

[18] V. F. Annese and D. De Venuto. "FPGA based architecture for fall-risk assessment during gait monitoring by synchronous EEG/EMG." Proceedings - 2015 6th IEEE International Workshop on Advances in Sensors and Interfaces, IWASI 2015, art. no. 7184953, pp. 116-121. DOI: 10.1109/IWASI.2015.7184953. 2015.

[19] D. De Venuto, V. F. Annese, M. Ruta, E. Di Sciascio, A. L. Sangiovanni Vincentelli. "Designing a Cyber-Physical System for Fall Prevention by Cortico-Muscular Coupling Detection.". IEEE Design and Test, 33 (3), art. no. 7273831, pp. 66-76. DOI: 10.1109/MDAT.2015.2480707. 2016.

[20] Y. Lajoie et al. "Predicting falls within the elderly community: Comparison of postural sway, reaction time, the Berg balance scale and the Activities-specific Balance Confidence (ABC) scale for comparing fallers and non-fallers", Arch. gerontology-geriatrics, 38.1:11-26, 2014.

[21] V. F. Annese, M. Crepaldi, D. Demarchi, D. De Venuto. "A digital processor architecture for combined EEG/EMG falling risk prediction". Proceedings of the 2016 Design, Automation and Test in Europe Conference and Exhibition, DATE 2016, art. no. 7459401, pp. 714-719. 2016.

[22] V. F. Annese and D. De Venuto. "The truth machine of involuntary movement: FPGA based cortico-muscular analysis for fall prevention" 2015 IEEE International Symposium on Signal Processing and Information Technology, ISSPIT 2015, art. no. 7394398, pp. 553-558. DOI: 10.1109/ISSPIT.2015.7394398. 2015.

[23] D. De Venuto, M. J. Ohletz, B. Ricco. "Automatic repositioning technique for digital cell based window comparators and implementation within mixed-signal DfT schemes". Proceedings - International Symposium on Quality Electronic Design, ISQED, 2003-January, art. no. 1194771, pp. 431-437. DOI: 10.1109/ISQED.2003.1194771. 2003.

[24] D. De Venuto, M.J. Ohletz, B. Riccò. "Digital window comparator DfT scheme for mixed-signal ICs" Journal of Electronic Testing: Theory and Applications (JETTA), 18 (2), pp. 121-128. DOI: 10.1023/A:1014937424827. 2002.

[25] V. F. Annese and D. De Venuto. "Fall-risk assessment by combined movement related potentials and co-contraction index monitoring". IEEE Biomedical Circuits and Systems Conference: Engineering for Healthy Minds and Able Bodies, BioCAS 2015 - Proceedings, art. no. 7348366. DOI: 10.1109/BioCAS.2015.7348366. 2015.

[26] R. P.Munhoz et al. "Evaluation of the pull test technique in assessing postural instability in Parkinson's disease." Neurology 62.1, 2004.

[27] Y. Han Bo, et al. "A low power ASIP for precision configurable FFT processing", Conf. Signal & Inform. Processing Association. 2012.

[28] D. De Venuto, S. Carrara, B. Riccò. "Design of an integrated low-noise read-out system for DNA capacitive sensors." Microelectronics Journal, 40 (9), pp. 1358-1365. DOI: 10.1016/j.mejo.2008.07.071. 2009.

[29] D. De Venuto, M. J. Ohletz, B. Riccò. "Testing of analogue circuits via (standard) digital gates". Proceedings - International Symposium on Quality Electronic Design, ISQED, 2002-January, art. no. 996709, pp. 112-119. DOI: 10.1109/ISQED.2002.9967097. 2002.

[30] D. De Venuto, M. J. Ohletz. "On-chip test for mixed-signal ASICs using two-mode comparators with bias-programmable reference voltages" (2001) Journal of Electronic Testing: Theory and Applications (JETTA), 17 (3-4), pp. 243-253. DOI: 10.1023/A:1013377811693. 2001.

[31] V. F. Annese and D. De Venuto. "Gait analysis for fall prediction using EMG triggered movement related potentials." Proceedings - 2015 10th IEEE International Conference on Design and Technology of Integrated Systems in Nanoscale Era, DTIS 2015, art. no. 7127386. DOI: 10.1109/DTIS.2015.7127386. 2015

[32] V. F. Annese, C. Martin, D. R. S. Cumming, D. De Venuto. "Wireless capsule technology: Remotely powered improved high-sensitive barometric endoradiosonde". Proceedings of 2016 IEEE International Symposium on Circuits and Systems (ISCAS) (pp. 1370-1373). DOI: 10.1109/ISCAS.2016.7527504. 2016, May. 2016.

[33] D. De Venuto, V. F. Annese, A. L. Sangiovanni-Vincentelli. "The ultimate IoT application: A cyber-physical system for ambient assisted living". Proceedings of *2016 IEEE International Symposium* on Circuits and Systems (ISCAS) (pp. 2042-2045). DOI: 10.1109/ISCAS.2016.7538979. 2016.

 ISBN: 978-1-61208-507-4